

Research Article

Investigation of Parameters Influencing Forming Force and Thickness Distribution in Single Point Incremental Forming of AA3105-St12 Two-Layer Sheet

H. Deilami Azodi^{1*}, S. Rezaei¹, A. Zeinolabedin Beygi² and H. Badparva³

¹ Department of Mechanical Engineering, Arak University of Technology, Arak, Iran

² Department of Mechanical Engineering, Tarbiat Modares University, Tehran, Iran

³ Department of Mechanical Engineering, Khajeh Nasir al-Din Tusi University of Technology, Tehran, Iran

ARTICLE INFO

Article history:

Received 6 February 2022

Reviewed 9 March 2022

Revised 20 March 2022

Accepted 3 April 2022

Keywords:

Single point incremental sheet forming

Two-layer sheet

Thickness distribution

Thinning

Forming force

ABSTRACT

Single point incremental sheet forming is a die-less forming technology in which the sheet metal is formed progressively by the movement of a tool in the specified path. In this paper, the single point incremental forming of the AA3105-St12 two-layer sheet is studied through numerical and experimental approaches. Numerical simulation of the process is done based on the finite element method. The validity of the numerical model is evaluated via a comparison between the obtained numerical and experimental results. The force applied to the forming tool, the thickness distribution of formed sheets, and the maximum thinning that occurred in aluminum and steel layers were studied. The effects of the parameters of the two-layer sheet including total thickness, thickness ratio of layers, and arrangement of layers were investigated as well. The results showed that regardless of the contact of the steel or aluminum layer with the tool, increasing the ratio of the thickness of the steel layer to the thickness of the aluminum layer reduces the thinning in the aluminum layer and increases it in the steel layer. Hence, thinning becomes more severe in each layer when it is in contact with the forming tool.

© Shiraz University, Shiraz, Iran, 2022

1. Introduction

Single point incremental sheet forming (SPISF) is a flexible forming technology in which the sheet metal is gradually formed by the movement of the tool in the specified path. Due to the progressive localized deformation of the sheet and concentration of the forces on the contact area of tool and sheet metal, the formability of the sheet increases in comparison with conventional forming methods [1]. Incremental sheet forming can be an economical forming process for batch production. Two-layer sheets have gained a wide range of

applications in fields of automotive, marine, aeronautical, and electrical industries due to their advantageous characteristics of being lightweight, corrosion resistant, and their electrical and thermal features. Various researches have been done on single-point incremental sheet forming. Hamilton et al. [2] investigated single point incremental forming (SPFI) of an ellipse at high rotational speeds and feed rates using the method of design of experiments (DOE). They studied the effects of process parameters on the surface quality, the thickness distribution, and the microstructure

* Corresponding author

E-mail address: hdazodi@arakut.ac.ir (H. Deilami Azodi)

<https://doi.org/10.22099/IJMF.2022.42993.1215>

of the part. They found that the thickness distribution and microstructure are similar to those of the low-speed condition. Kim et al. [3], assuming shear deformation in single point incremental forming process, calculated the thickness distribution for asymmetric shapes. They introduced a two-step process in which the less deformed areas in the second step are deformed a lot in the first step and vice versa. They showed that with this two-step process instead of a one-step, the thickness distribution is improved and the formability increases. Mirmia et al. [4] by presenting a new three-step deformation strategy for SPIF of an aluminum cone with a wall angle of 70° , reduced the thinning from 74% in the one-step state to 51%. That was the least amount of thinning occurred compared to the previous strategies. Chang et al. [5] developed analytical models to predict the forces in various directions in single-pass/single point incremental forming (SPIF), multi-pass incremental forming (MPIF), and incremental hole flanging (IHF) processes. The mechanism of force fluctuation was also investigated and showed that it is caused by varied elastic deflection of the deforming sheet. Feng et al. [6] investigated the electromagnetic incremental forming large-sized sheets on multi-point dies. A multi-point die can form different curves on a sheet. The results showed that the maximum stress has an inverse ratio with the curved radius. Manco et al. [7] used the method of design of experiments to investigate the effects of tool diameter, vertical pitch size, sheet thickness, and wall angle on the minimum thickness in the incremental forming of an AA6082 cone. Based on the relationship resulting from the experimental data, the diameter of the tool has no significant effect on the minimum thickness. As the vertical pitch increases, the minimum thickness increases. Young et al. [8] investigated the two-step SPIF of a cone, experimentally. The two-step process increases the formability by delaying the formation of areas with excessive thinning. This strategy did not reduce the thinning but changed the location of thinning in a 70° cone. Duflou et al. [9] investigated the SPIF of a cylindrical part in five steps experimentally. They designed the intermediate shapes by increasing the wall angle by 10° in each step. They suggested the use of

multi-step forming as a way to delay premature thinning instead of one-step incremental forming. Duflou et al. [10] provided an exhaustive overview of research achievements in single-point incremental forming. Scientific progress in the field and outlook on expected further developments has been reviewed. Skjoedt et al. [11] investigated the effect of the direction of tool movement between consecutive steps in single point incremental forming a cylindrical part on the strain distribution and the final thickness variation, experimentally and numerically. They concluded that the experimentally determined FFLCs can successfully be employed to establish the forming limits of multi-stage SPIF. Zhang et al. [12] proposed a multi-step strategy for SPIF. They studied the behavior of the forming process and the thickness distribution. Numerical simulation of hydraulic bulging was used to obtain intermediate shapes. They concluded that the forming limit of the sheet can be improved by imitating the approach between intermediate surfaces. Kumar et al. [13] investigated and optimized the parameters of the single-point incremental forming process. Seven parameters affecting the process were optimized using the DOE method to minimize the forming force and thickness reduction. Esmaeilpour et al. [14] utilized three-dimensional (3D) yield functions to account for normal and shear stress components in incremental sheet forming processes. They used three different yield functions von Mises, Hill's 1948, and Barlat Yld2004-18p to simulate the single point incremental forming (SPIF) of 7075-O aluminum alloy sheet by finite element method. The effective plastic strain distribution, part thickness, tool force and moment, and stress and strain components predicted by simulations based on various yield functions were compared. Pak et al. [15] studied the effect of ultrasonic vibration applied to the tool in single point incremental sheet metal forming process. An analytical model was developed to predict the forming force in the case of applying ultrasonic vibration. The experimental study was also carried out for practical evaluation of applying ultrasonic vibration to the tool in SPIF. Results showed that the forming force in the case of applying ultrasonic vibration dramatically reduced

compared to the normal mode. Deilami Azodi et al. [16] studied the incremental forming of the AA3105-St12 two-layer sheet, numerically and experimentally, to calculate the forming force and final thicknesses of the layers. They developed the numerical models for estimating the vertical force applied on the tool and the final thicknesses of the layers using artificial neural network. Multi-objective optimization was carried out to obtain minimum forming force and minimum thickness reduction of layers. Ullah et al. [17] studied the geometric accuracy in double-sided incremental forming with various tool path strategies. They discussed tool path generating procedure, thickness distribution, deformation, and fracture mechanism for double-sided incremental forming. Kumar et al. [18] investigated the formability of tailor laminated sheets of aluminum alloy AA5083 and polycarbonate in single point incremental forming (SPIF) using the forming limit curve (FLC). They determined the maximum achievable wall angle through forming the sheet into square pyramid shapes. Ghorbani et al. [19] studied the two-point incremental forming-machining process. The process involved machining and incremental forming of planar and twisted AA5083 blades. They used a feature-based algorithm to design the tool path. The dimensional accuracy of the final product was enhanced. They concluded that the deformation machining process (DMP) can be used to fabricate complex curved-surface

work pieces with acceptable dimensional accuracy.

In the present work, the single point incremental forming of the AA3105-St12 two-layer sheet is investigated experimentally and numerically. The force applied to the forming tool, the thickness distribution of formed sheets, and the maximum thinning that occurred in aluminum and steel layers are studied. Numerical results are compared with experimental ones to examine the validity of the numerical approach. The effects of the thickness ratio of layers, total thickness of two-layer sheets, the arrangement of layers on the forming force, thickness distribution, and thinning are investigated in the present study.

2. Experimental Procedure

Experiments were carried out on two-layer sheets consisting of 0.5 mm thickness aluminum alloy AA13105 sheets and 0.5 mm thickness carbon steel St12. Mechanical properties of the layers are determined using the uniaxial tensile tests. Assuming the power-law hardening rule ($\sigma = k\varepsilon^n$), mechanical properties of used sheets are listed in Table 1. The chemical composition of carbon steel and aluminum alloy sheets are given in Tables 2 and 3, respectively. Polyurethane adhesive was used to join two layers. The final part, as shown schematically in Fig. 1, was a truncated cone with a large diameter of 40 mm, a height of 23 mm, and a wall angle of 35°.

Table 1. Mechanical properties of Al3105 and St12 sheets

Variables	Values	
	St-12	Al 3105
Material	St-12	Al 3105
Thickness, t (mm)	0.5	0.5
Young's modulus, E (MPa)	210000	70000
Poisson's ratio	0.3	0.33
Density, (kg/m ³)	7850	2700
Strength coefficient, K^* (MPa)	510	302
Strain hardening exponent, n^*	0.2	0.103

Table 2. Chemical composition of carbon steel St12 steel sheet [20]

Element	Si	Fe	Cu	Mn	Mo	C	W	Nb	B	Cr	Ni	Al
Weight percentage	0.027	98.46	0.053	0.66	0.005	0.24	0.024	0.043	0.048	0.046	0.02	0.036

Table 3. Chemical composition of aluminum alloy AA3105 Al sheet [21]

Element	Si	Fe	Cu	Mn	Mg	Zn	Ti	Cr	Ni	Al
Weight percentage	0.298	0.629	0.044	0.437	0.350	0.025	0.018	0.022	0.013	98.160

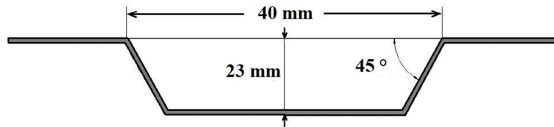


Fig. 1. Schematic of the final part.

Single point incremental forming of two-layer specimens was performed on a numerical control milling machine, model FP4MK, made by MST company. A fixture with working dimensions of 125 mm x 170 mm x 170 mm was used to clamp the specimens. The experimental setup is shown in Fig. 2. A non-rotational spherical head incremental forming tool was employed to form the specimens. This forming tool consists of a 10 mm diameter hardened ball of chrome steel alloy AISA 52100 connected to a steel shank with a diameter of 10 mm. The feed rate and incremental depth of the tools in all experiments were 0.03 m/s and 1 mm, respectively. Fig. 3 shows samples of formed specimens.

3. Numerical Simulation

Finite element simulation of single point incremental forming of the two-layer sheet was performed with ABAQUS/Explicit code. Modeling of a two-layer sheet made of aluminum alloy AA13105 and carbon steel St12 layers is done with mechanical properties determined in an experimental study (Table 1). The two-layer sheet was modeled as a three-dimensional deformable part with

4-node and 3-node shell elements (S4R & S3R), while the forming tool was modeled as a discrete rigid body with R3D4 elements. The total element number of the sheet was 8626, including 7524 elements of 4-node type and 1102 elements of 3-node type. It was assumed that there was no slipping among layers, so the tie constraint was used between two layers. During the analysis, the amount of kinetic energy and internal energy were checked continuously to ensure the validity of the quasi-static state. Clamping of the sheet via fixture was modeled by fixing all degrees of freedom of the edges of the sheet. The Coulomb friction model with a constant friction coefficient of 0.1 [22] was used at the contact point between the forming tool and the sheet. The geometry of the final part was similar to experimental tests, as shown in Fig. 1. The tool path is considered a circle with a fixed vertical step and parameters similar to experimental tests. A deformed sheet in the numerical simulation is shown in Fig. 4.

Single point incremental forming of the St12-AA3105 two-layer sheet was simulated with different values of total thickness and thickness ratio of layers, as well as in different cases of contact of the aluminum layer or steel layer with the forming tool. The thickness ratio is defined as the ratio of the thickness of the top layer (the layer is in contact with the forming tool) to the thickness of the bottom layer. Table 4 shows the total of 18 different states of the process that were simulated.



Fig. 2. Experimental setup.



Fig. 3. Samples of formed specimens.

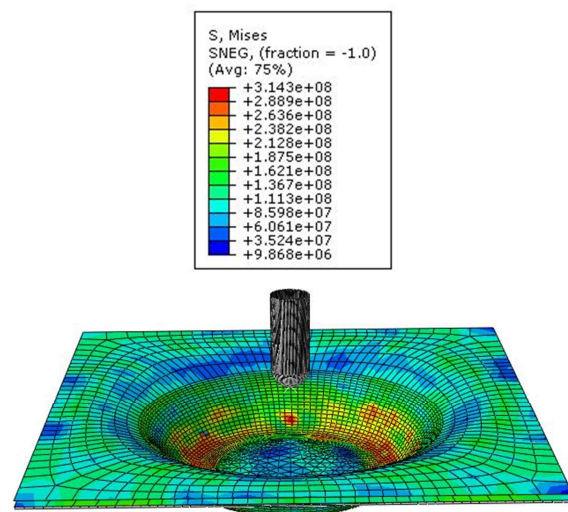


Fig. 4. A sheet formed in finite element simulation.

Table 4. Possible states of process with full factorial approaching

No	Thickness Ratio	Total Thickness (mm)	Thickness, Al (mm)	Thickness, St (mm)	Arrangement
1	2	3	1	2	SA
2	0.5	2	0.6666667	1.3333333	AS
3	0.5	2	1.3333333	0.6666667	SA
4	0.5	3	1	2	AS
5	2	2	1.3333333	0.6666667	AS
6	1	1	0.5	0.5	AS
7	2	1	0.6666667	0.3333333	AS
8	1	3	1.5	1.5	SA
9	2	3	2	1	AS
10	0.5	1	0.3333333	0.6666667	AS
11	2	2	0.6666667	1.3333333	SA
12	1	3	1.5	1.5	AS
13	2	1	0.3333333	0.6666667	SA
14	0.5	1	0.6666667	0.3333333	SA
15	0.5	3	2	1	SA
16	1	2	1	1	AS
17	1	1	0.5	0.5	SA
18	1	2	1	1	SA

Design of experiment (DOE) method with the full factorial technique was used to determine the test's condition. "AS" stands for the condition in which the aluminum layer is in contact with the forming tool, but on the contrary, "SA" represents the steel layer is in contact with the forming tool.

4. Results and Discussion

4.1. Validation of numerical simulation

The distribution of the final thickness of the layers obtained numerically has been compared with experimental ones to verify the validity of the numerical simulation. Fig. 5 shows the thickness measurement path in a cut sample. Comparisons of the thickness distributions obtained from the numerical and experimental approaches for aluminum and steel layers are presented in Figs. 6 and 7 in AS and SA cases, respectively. It can be seen that the numerical results are in good agreement with those obtained from real experiments.

4.2. Forming force

Fig. 8 shows the force applied to the forming tool measured in experiments for two different arrangements of layers. While moving the tool, the forming force initially increases due to the strain hardening effect. As



Fig. 5. Thickness measurement path.

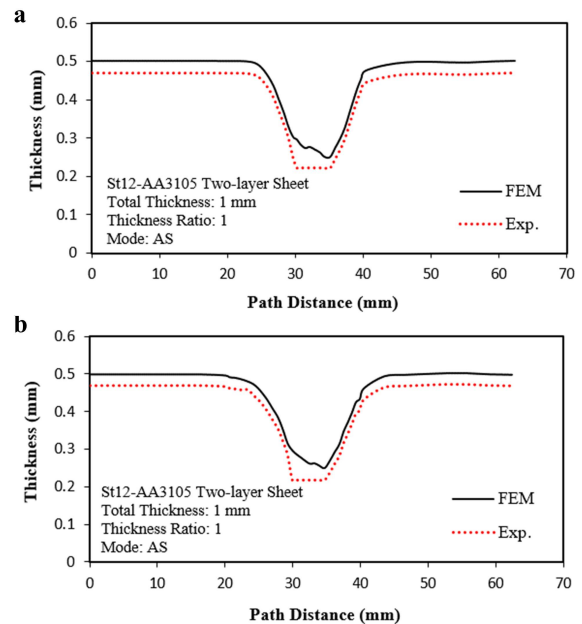


Fig. 6. Comparisons of the thickness distributions obtained from the numerical and experimental approaches for (a) aluminum layer and (b) steel layer in the case of contact of the aluminum layer with the forming tool (Mode AS).

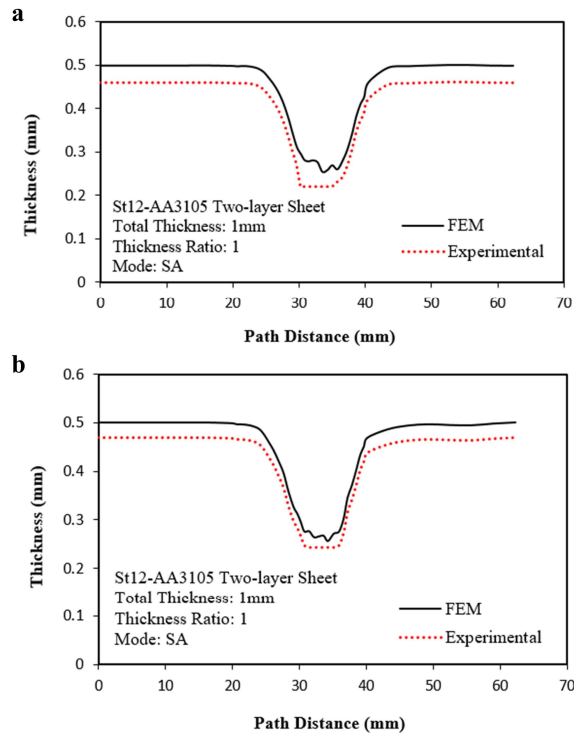


Fig. 7. Comparisons of the thickness distributions obtained from the numerical and experimental approaches for (a) aluminum layer and (b) steel layer in the case of contact of the steel layer with the forming tool (Mode SA).

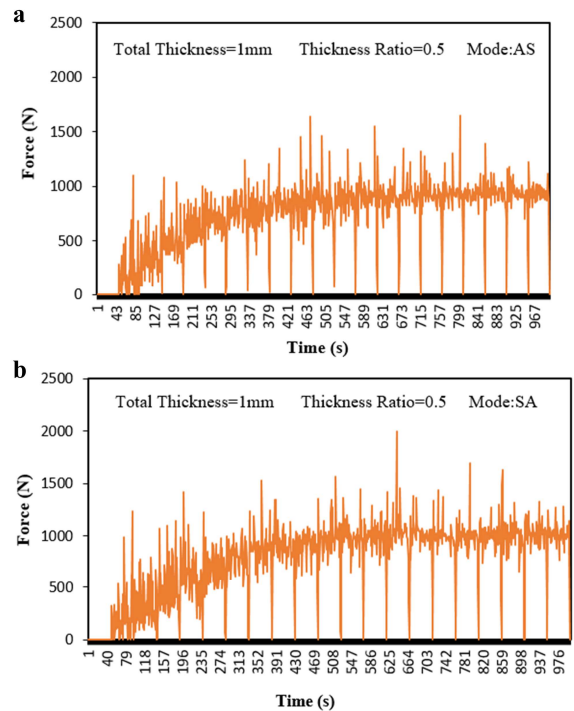


Fig. 8. Force applied to the forming tool measured in experiments in (a) mode AS and (b) mode SA.

the forming continues, the force applied to the tool remains almost constant. It seems that the balance between increasing the force due to the strain hardening and decreasing the force due to the thinning of the sheet is the reason the force remains constant.

Figs. 9 to 11 show the effect of the thickness ratio on the force applied to the forming tool for the different amounts of the total thickness of the two-layer sheet and different arrangements of layers. It can be concluded that in the case of AS, the forming force decreases by increasing the thickness ratio. In the case of SA, increasing the thickness ratio rises the forming tool.

Since the thickness ratio is defined as the ratio of the thickness of the top layer (the layer is in contact with the forming tool) to the thickness of the bottom layer, both decreasing the thickness ratio in mode AS and increasing it in mode SA mean increasing the ratio of the thickness of steel layer to the thickness of aluminum layer; Hence, both of them lead to an increase in the force applied to the tool.

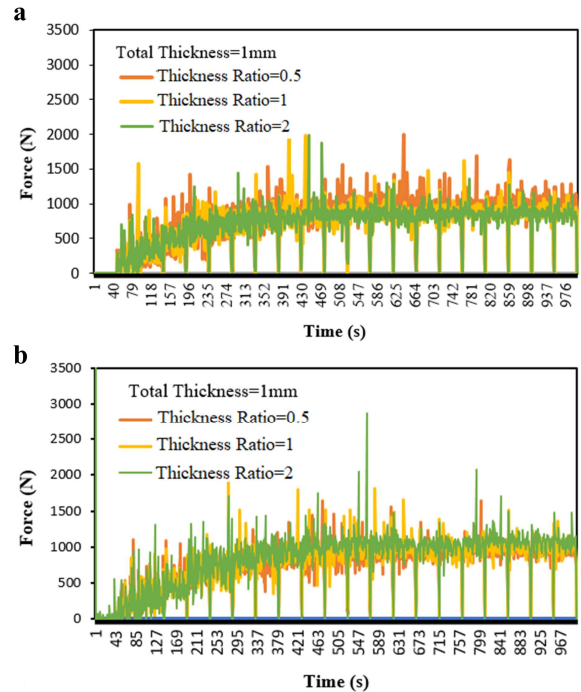


Fig. 9. The effect of the thickness ratio on the forming force for the total thickness of 1 mm in (a) mode AS and (b) mode SA.

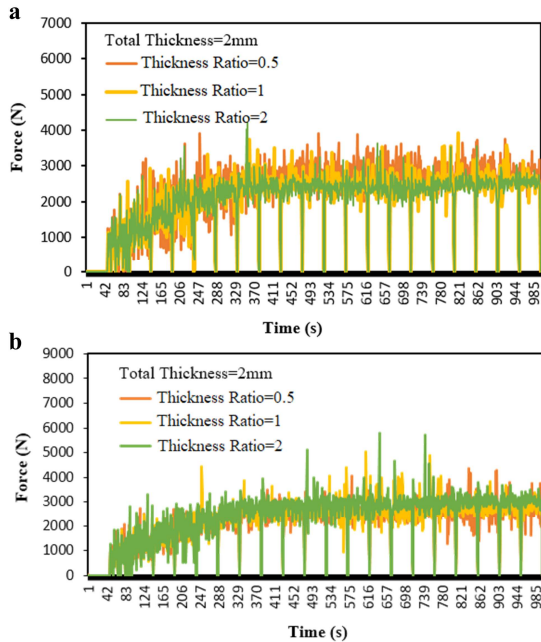


Fig. 10. The effect of the thickness ratio on the forming force for the total thickness of 2 mm in (a) mode AS and (b) mode SA.

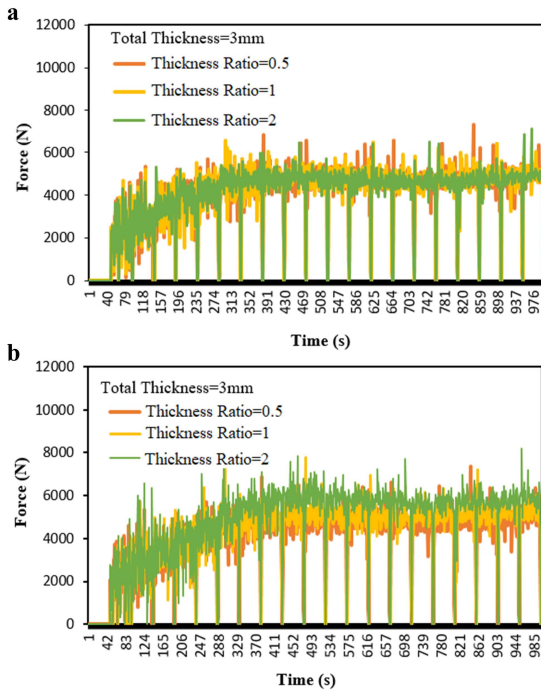


Fig. 11. The effect of the thickness ratio on the forming force for the total thickness of 3 mm in a) mode AS and b) mode SA.

Figs. 12 to 14 show the effect of the total thickness of the two-layer sheet on the forming force for the different thickness ratios and different arrangements of layers. As expected, in a specified thickness ratio, the force applied to the forming tool rises by increasing the total thickness of the two-layer sheet.

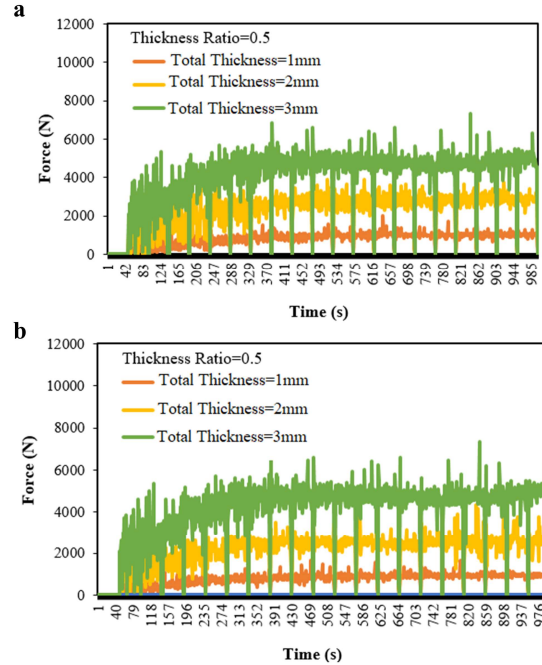


Fig. 12. The effect of the total thickness on the forming force for the thickness ratio of 0.5 in (a) mode AS and (b) mode SA.

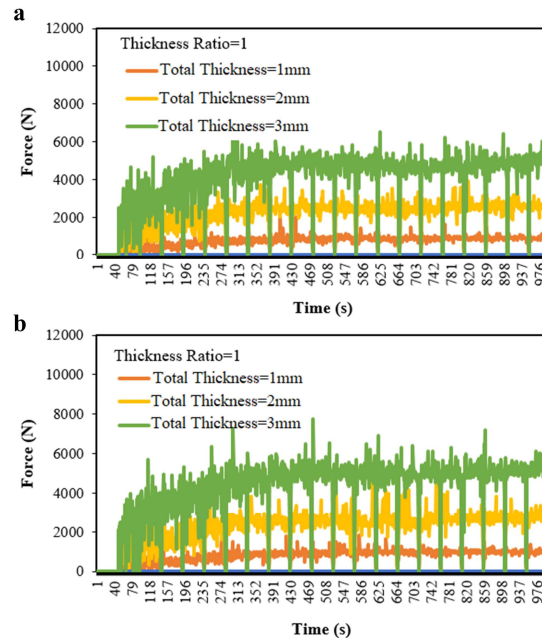


Fig. 13. The effect of the total thickness on the forming force for the thickness ratio of 1 in (a) mode AS and (b) mode SA.

4.3. Thickness distribution and thinning

The thickness distribution of AA3105 and St12 layers are shown in Figs. 15 to 20 for the different total thicknesses and arrangements of layers and the effects of the thickness ratio on thickness variation and thinning are investigated. According to the results shown in the figures,

in the case of AS increasing the thickness, ratio causes more severe thinning in the aluminum layer and reduces thinning in the steel layer. It is also seen in the case of SA that increasing the thickness ratio leads to less thinning in the aluminum layer and more thinning in the steel one.

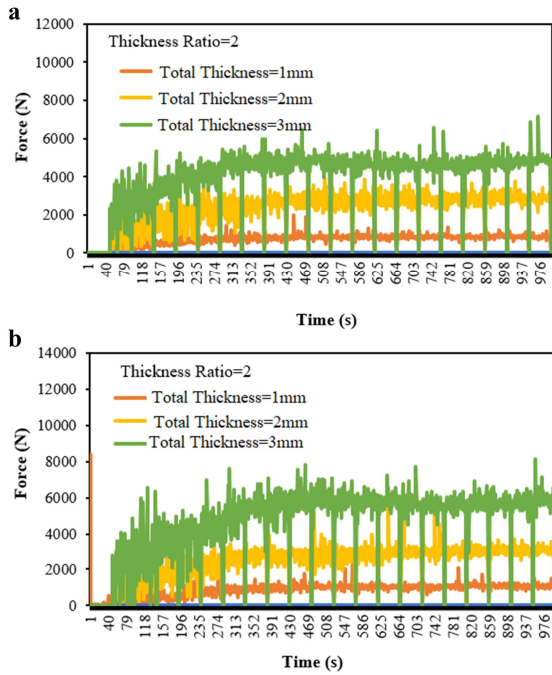


Fig. 14. The effect of the total thickness on the forming force for the thickness ratio of 2 in (a) mode AS and (b) mode SA.

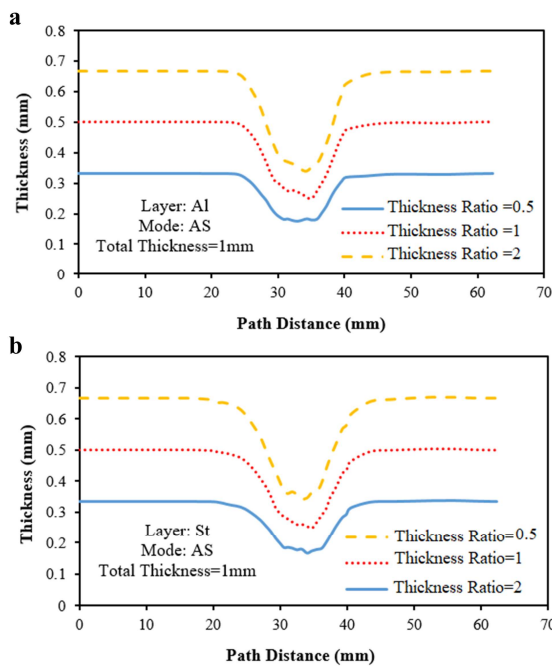


Fig. 15. The effect of the thickness ratio on thickness distribution of (a) aluminum layer and (b) steel layer for the total thickness of 1 mm in mode AS.

The maximum thinning that occurred in each layer can be determined according to the initial thickness of the layer and the minimum thickness after forming. Percentages of thinning in aluminum and steel layers for different total thicknesses and thickness ratios in AS and SA modes are represented in Figs. 21 and 22.

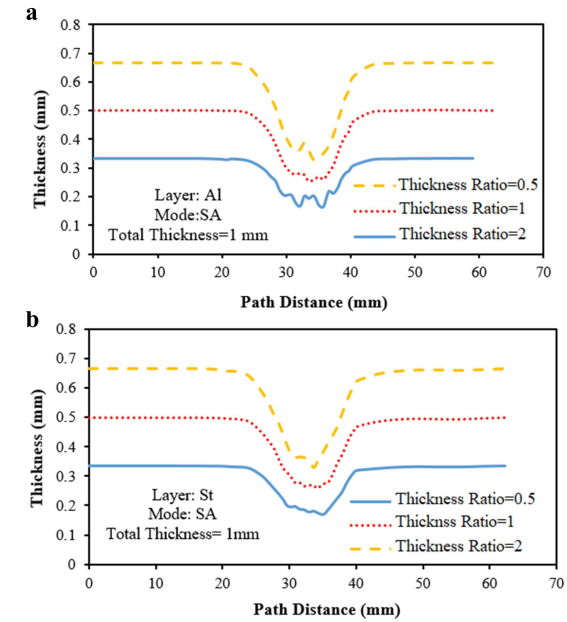


Fig. 16. The effect of the thickness ratio on thickness distribution of (a) aluminum layer and (b) steel layer for the total thickness of 1 mm in mode SA.

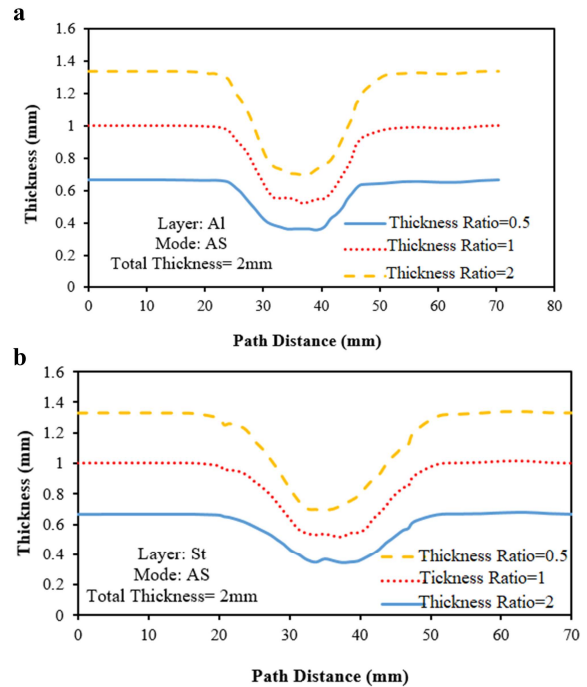


Fig. 17. The effect of the thickness ratio on thickness distribution of (a) aluminum layer and (b) steel layer for the total thickness of 2 mm in mode AS.

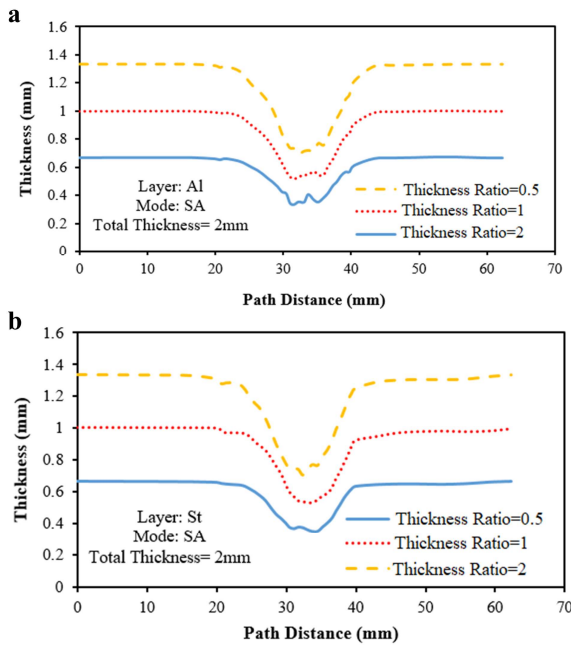


Fig. 18. The effect of the thickness ratio on thickness distribution of (a) aluminum layer and (b) steel layer for the total thickness of 2 mm in mode SA.

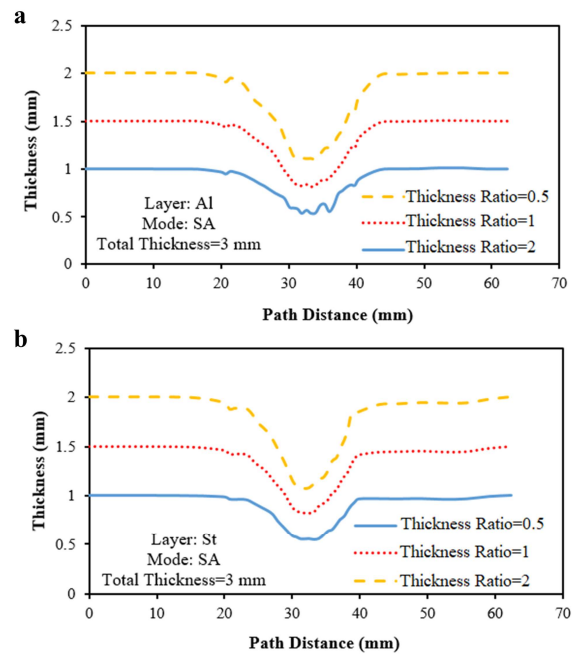


Fig. 20. The effect of the thickness ratio on thickness distribution of (a) aluminum layer and (b) steel layer for the total thickness of 3 mm in mode SA.

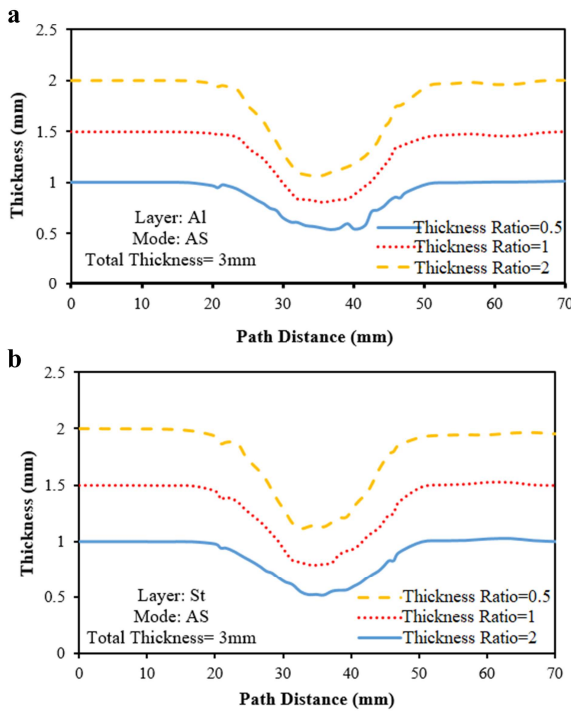


Fig. 19. The effect of the thickness ratio on thickness distribution of (a) aluminum layer and (b) steel layer for the total thickness of 3 mm in mode AS.

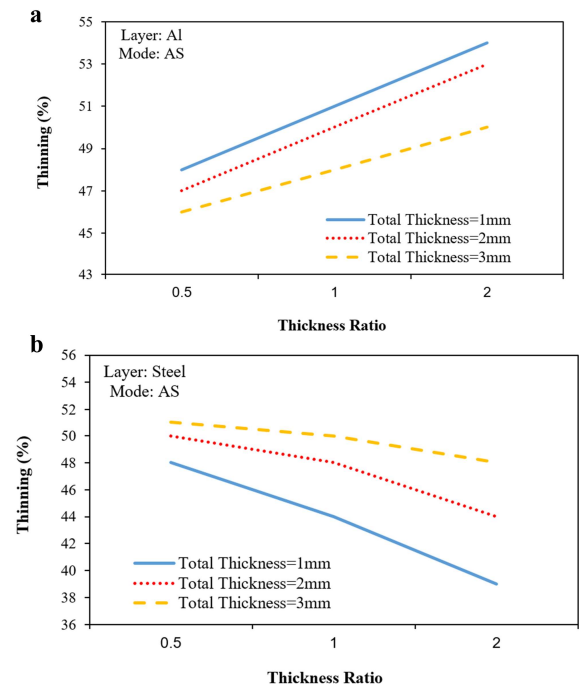


Fig. 21. Percent thinning in (a) aluminum layer and (b) steel layers in mode AS.

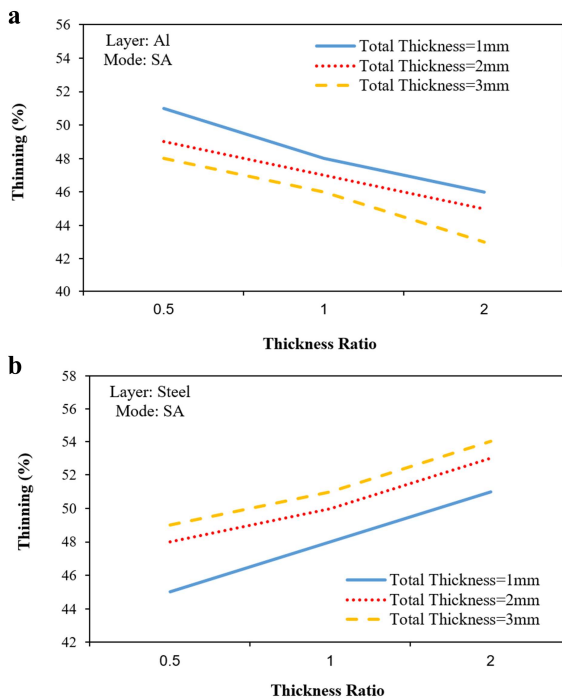


Fig. 22. Percent thinning in (a) aluminum layer and (b) steel layers in mode SA.

The thickness ratio is the ratio of the thickness of the top layer to the thickness of the bottom layer; hence, decreasing the thickness ratio in mode AS and increasing it in mode SA means increasing the ratio of the thickness of the steel layer to the thickness of the aluminum layer (t_{St}/t_{Al}). Therefore, it can be concluded that regardless of the contact of the steel or aluminum layer with the tool (mode AS or SA), increasing the ratio of the thickness of the steel layer to the thickness of the aluminum layer reduces the thinning in the aluminum layer and causes more thinning in the steel layer. It means that by using the higher values of (t_{St}/t_{Al}) the amount of the minimum thickness in the aluminum layer will increase and the minimum thickness value in the steel layer will reduce.

Figs. 23 to 25 show the effect of the arrangement of the layers on the percentage of thinning occurring in aluminum and steel layers. To evaluate the effect of layer arrangement on maximum thinning, the thinning values are compared at the same ratio of steel layer thickness to the aluminum layer thickness, and only the layer in contact with the tool is changed.

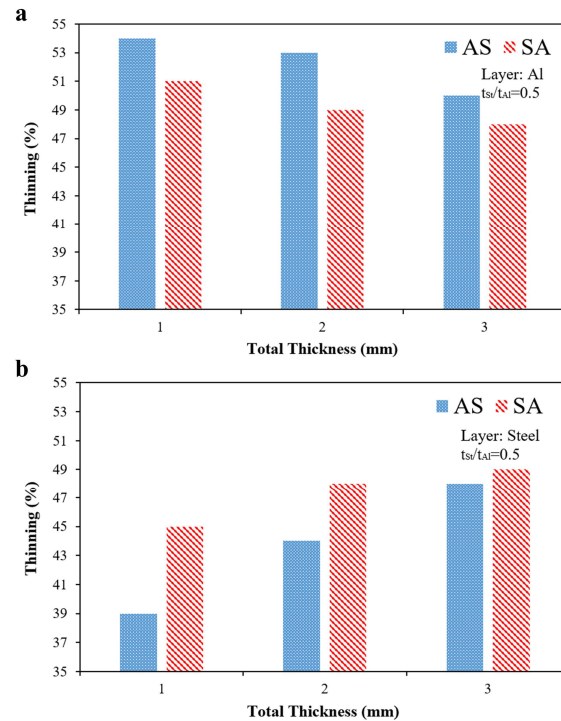


Fig. 23. The effect of the arrangement of the layers on maximum thinning in (a) aluminum (b) steel layers for $t_{St}/t_{Al} = 0.5$.

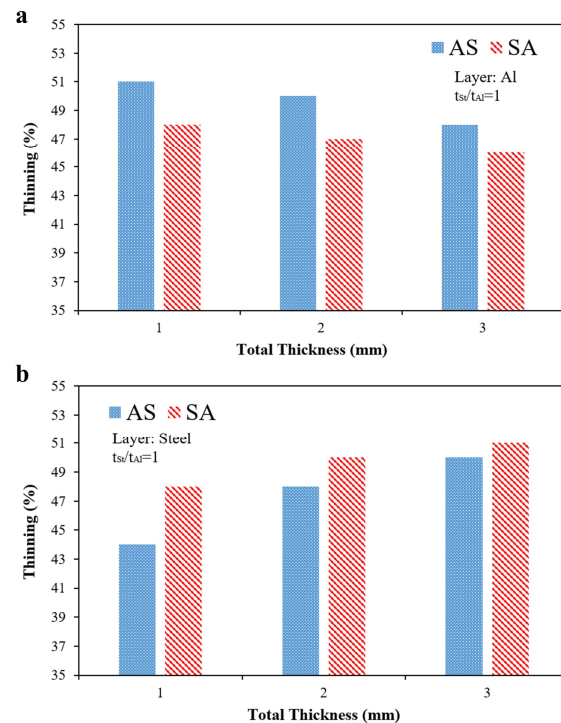


Fig. 24. The effect of the arrangement of the layers on maximum thinning in (a) aluminum (b) steel layers for $t_{St}/t_{Al} = 1$.

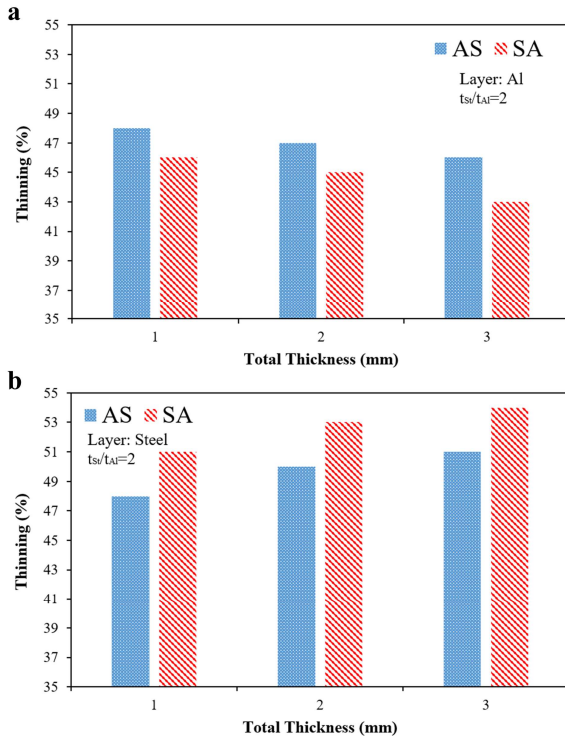


Fig. 25. The effect of the arrangement of the layers on maximum thinning in (a) aluminum (b) steel layers for $t_{St}/t_{Al} = 2$.

The diagrams indicate that the maximum thinning of the aluminum layer in mode AS is greater than in mode SA; conversely, in the steel layer, more thinning occurs in the SA mode. So, it can be concluded that the maximum thinning in each layer is greater when it is in contact with the forming tool.

5. Conclusion

In this paper, the single point incremental forming of the AA3105-St12 two-layer sheet was studied numerically using the finite element simulation. Experiments were also done to verify the validity of the numerical simulations. Numerical and experimental distribution of the final thickness of the layers were compared and a good agreement was seen between them. The influences of the thickness ratio of layers, total thickness of the two-layer sheet, and arrangement of layers on the forming force, thickness distribution, and thinning were also investigated. The following conclusions can be drawn:

- Increasing the ratio of the thickness of the steel layer

to the thickness of the aluminum layer increases the force applied to the forming tool.

- The force applied to the forming tool increases by increasing the total thickness of the two-layer sheet.
- Increasing the thickness ratio causes more thinning in the aluminum layer and reduces thinning in the steel layer in mode AS. Whereas in the case of SA, increasing the thickness ratio reduces the thinning in the aluminum layer and leads to more thinning in the steel layer.
- Higher values for the ratio of the thickness of the steel layer to the thickness of the aluminum layer causes less thinning in the aluminum layer and more thinning in the steel layer in both AS and SA modes.
- The thinning occurred in aluminum and steel layers become more severe when they are in contact with the forming tool.

Acknowledgments

The authors acknowledge Arak University of Technology for providing supports during the research work.

Conflict of Interests

The authors declare that they have no conflict of interest.

6. References

- [1] A. Peteka, B. Jurisevic, K. Kuzman, M. Junkar, Comparison of alternative approaches of single point incremental forming processes, *Journal of Materials Processing Technology*, 209(4) (2009) 1810-1815.
- [2] K. Hamilton, J. Jeswiet, Single point incremental forming at high feed rates and rotational speeds: Surface and structural consequences, *CIRP Annals*, 59(1) (2010) 311-314.
- [3] T.J. Kim, D.Y. Yang, Improvement of formability for the incremental sheet metal forming process, *International Journal of Mechanical Science*, 42(7) (2000) 1271-1286.
- [4] M.J. Mirnia, D. Mollaei Dariani, H. Vanhove, J.R. Dufloy, Thickness improvement in single point incremental forming deduced by sequential limit

- analysis, *International Journal of Advanced Manufacturing Technology*, 70(9) (2014) 2029-2041.
- [5] Z. Chang, M. Li, J. Chen, Analytical modeling and experimental validation of the forming force in several typical incremental sheet forming processes, *International Journal of Machine Tools and Manufacture*, 140 (2019) 62-76.
- [6] F. Feng, J. Li, R. Chen, L. Huang, H. Su, S. Fan, Multi-point die electromagnetic incremental forming for large-sized sheet metals, *Journal of Manufacturing Processes*, 62 (2021) 458-470.
- [7] G.L. Manco, G. Ambrogio, Influence of thickness on formability in 6082-T6, *International Journal of Material Forming*, 3(1) (2010) 983- 986.
- [8] D. Young, J. Jeswiet, Wall thickness variations in single-point incremental forming, *Proceedings of the Institution of Mechanical Engineers, Part B: Journal of Engineering Manufacture*, 218(11) (2004) 1453-1459.
- [9] J.R. Dufloy, J. Verbert, B. Belkassen, J. Gu J, H. Sol, C. Henrard, A.M. Habraken, Process window enhancement for single point incremental forming through multi-step toolpaths, *CIRP Annals*, 57(1) (2008) 253-256.
- [10] J.R. Dufloy, A.M. Habraken, J. Cao, R. Malhotra, M. Bambach, D. Adams, H. Vanhove, A. Mohammadi, J. Jeswiet, Single point incremental forming: state-of-the-art and prospects, *International Journal of Material Forming*, 11(6) (2018) 743-773.
- [11] M. Skjoedt, M.B. Silva, P.A.F. Martins, N. Bay, Strategies and limits in multi-stage single-point incremental forming, *The Journal of Strain Analysis for Engineering Design*, 45(1) (2010) 33-44.
- [12] C. Zhang, H.F. Xiao, D.H. Yu, Incremental forming path-generated method based on the intermediate models of bulging simulation, *The International Journal of Advanced Manufacturing Technology*, 67(9) (2013) 2837-2844.
- [13] A. Kumar, V. Gulati, Optimization and investigation of process parameters in single point incremental forming, *Indian Journal of Engineering and Materials Sciences (IJEMS)*, 27(2) (2021) 246-255.
- [14] R. Esmailpour, H. Kim, T. Park, F. Pourboghra, B. Mohammed, Comparison of 3D yield functions for finite element simulation of single point incremental forming (SPIF) of aluminum 7075, *International Journal of Mechanical Sciences*, 133 (2017) 544-554.
- [15] A. Pak, H. Deilami Azodi, M. Mahmoudi, Investigation of ultrasonic assisted incremental sheet metal forming process, *Modares Mechanical Engineering*, 14(11) (2015) 106-114.
- [16] H. Deilami Azodi, S. Rezaei, H. Badparva, A. Zeinolabedin Beygi, Optimizing AA3105-St12 two-layer sheet in incremental sheet forming process using neural network and multi-objective genetic algorithm, *Modares Mechanical Engineering*, 22(2) (2022) 121-132.
- [17] S. Ullah, P. Xu, X. Li, Y. Li, K. Han, D. Li, A review on part geometric precision improvement strategies in double-sided incremental forming, *Metals*, 12(1)(2022) 103.
- [18] G. Kumar, K. Maji, Investigations on formability of tailor laminated sheets in single point incremental forming, *Proceedings of the Institution of Mechanical Engineers, Part B: Journal of Engineering Manufacture*, (2022) 09544054221076244.
- [19] H. Ghorbani-Menghari, M. Azadipour, M. Ghasempour-Mouziraji, Y. Hoon Moon, J. Hoon Kim, Effect of process parameters on formability in two-point incremental forming-machining of planar and twisted AA5083 blades, *Proceedings of the Institution of Mechanical Engineers, Part B: Journal of Engineering Manufacture*, (2022) 09544054211069743.
- [20] V. Alimirzaloo, M. Abdollahzadeh Gavgani, S. Ahmadi, A. Donyavi, Investigation of the effective factors on strain distribution in round section roll forming process using the design of experiments, *Amirkabir Journal of Mechanical Engineering*, 49(2) (2017) 413-422.
- [21] O. Zubillaga, F.J. Cano, I. Azkarate, I.S. Molchan, G.E. Thompson, A.M. Cabral, P.J. Morais, Corrosion performance of anodic films containing polyaniline and TiO₂ nanoparticles on AA3105 aluminium alloy, *Surface and Coatings Technology*, 202(24) (2008) 5936-5942.
- [22] J.C. Li, L.I. Chong, T.G. Zhou, Thickness distribution and mechanical property of sheet metal incremental forming based on numerical simulation, *Transactions of Nonferrous Metals Society of China*, 22 (2012) 54-60.